

5.2 SPACEBORNE CLIMATE CHANGE MONITORING BY GNSS OCCULTATION SENSORS

Gottfried Kirchengast^{1)*}, Andrea K. Steiner¹⁾, Ulrich Foelsche¹⁾,
Luis Kornblueh²⁾, Elisa Manzini²⁾, and Lennart Bengtsson²⁾,
¹⁾Inst. for Meteorology and Geophysics, Univ. of Graz, Graz, Austria
²⁾Max-Planck-Institute for Meteorology, Hamburg, Germany

1. INTRODUCTION

The monitoring of climate change, especially of atmospheric change, over the coming decades is highly relevant in view of concerns that the evolution of the Earth's climate system is increasingly influenced by human activities (e.g., IPCC 1995). Considerable efforts are thus currently invested into the setup of a Global Climate Observing System (GCOS), which shall enable significant advances in understanding and predicting climate variability and in detecting anthropogenic climate impacts (e.g., JSTC-GCOS 1998).

A very promising observing system in this context is a suite of spaceborne Global Navigation Satellite System (GPS and GLONASS, generically GNSS) occultation sensors, which holds potential to become a leading backbone of GCOS for global long-term monitoring of atmospheric change in temperature and other variables with unprecedented accuracy.

The GNSS occultation technique is an active limb sounding technique exploiting trans-atmospheric satellite-to-satellite radio links. The method became recently feasible due to the installation of the GNSS with its high-precision L band navigation signals near 1.6 GHz (L1) and 1.2 GHz (L2), respectively (e.g., Gurvich and Krasil'nikova 1990; Ware et al. 1996).

The principal observable, measured with millimetric precision, is the excess phase path (relative to propagation in vacuum) of the GNSS-transmitted radio waves caused by refraction during passage through the atmosphere in occultation geometry (e.g., Kursinski et al. 1997). In this way, GNSS occultation sensors probe refractive properties of the atmosphere and profiles of associated fundamental atmospheric variables such as temperature and humidity can be retrieved with high quality (e.g., Steiner et al. 1999).

Despite the promise, the climate change monitoring utility of a GNSS occultation observing system has not yet been tested in any rigorous quantitative manner, the main reason being the complexity of the issue given the current lack of real data for such a study.

We are currently performing a rigorous study that copes with this complexity using an end-to-end GNSS occultation observing system simulation experiment over the 25-year period 1996 to 2020. In this paper we mainly report, based on the current status (Sep. 1999),

* *Corresponding author address:* Gottfried Kirchengast, Institute for Meteorology and Geophysics, University of Graz, Halbaerthgasse 1, A-8010 Graz, Austria; e-mail: gottfried.kirchengast@kfunigraz.ac.at.

on the first phase of setting up the study design and the required tools.

We start the report with a brief outline of the potential of GNSS occultation for climate monitoring (section 2) before we describe design and tools (section 3). A summary (section 4) concludes the paper.

2. POTENTIAL FOR CLIMATE MONITORING

The GNSS occultation method bears considerable potential for climate variability and change studies in providing a unique combination of global coverage, high vertical resolution and accuracy, long-term stability, and all-weather capability (e.g., Kursinski et al. 1997).

Of particular importance to climate studies is the exceptional long-term stability, which derives from the self-calibrating nature of the radio occultation technique, where phase change is measured (instead of radiance). This is very accurately possible using the highly stable GNSS signals and readily available precise clocks. Measurements from different satellites and times can thus be included in a climate dataset without any adjustments.

The greatest strength of the method is the profiling of the thermal structure (temperature profiling) in the upper troposphere and stratosphere. Indications exist that the changing thermal structure in this domain is a particularly sensitive indicator of anthropogenic climate impacts due to increased greenhouse gas emissions (IPCC 1995). We expect that GNSS occultation sensors can furnish data to globally monitor this changing structure with a quality surpassing any comparable observations.

Further promising climate change indicators accessible by the technique are the geopotential structure over the same vertical domain as temperature and the humidity structure in the lower and middle troposphere (Kursinski et al. 1997).

This study focuses on assessing the utility of GNSS-derived temperature climatologies for detecting anthropogenic influences.

3. STUDY DESIGN AND TOOLS

Based on an approach, which can be termed a "climate observing system simulation experiment", we perform a rigorous quantitative test of the climate change detection capability of GNSS occultation sensors by an integrated analysis involving five main parts of work as follows.

(i) Realistic modeling of the atmosphere (neutral atmosphere and ionosphere) over the time period 1996 to 2020.

(ii) Realistic simulations of occultation observables (i.p. of excess phase path profiles) for a small constellation of GNSS occultation sensors for 1996 to 2020.

(iii) State-of-the-art data processing for temperature profile retrieval in the troposphere and stratosphere to establish a sufficient database of realistic simulated temperature measurements for 1996 to 2020.

(iv) A multivariate statistical analysis of temperature trends in both the “measured” climatology based on the database of simulated measurements and the “true” climatology from the atmosphere modeling.

(v) An assessment, by statistical inference, of whether and to what degree the GNSS occultation observing system is able to detect anthropogenic climatic trends in the atmospheric evolution.

Each of these work parts (i) – (v) is briefly described in the subsections below.

3.1 Atmosphere and Ionosphere Modeling

Both the neutral atmosphere and the ionosphere need to be adequately modeled globally from 1996 to 2020, the latter in order to properly capture ionospheric residual errors in retrieved atmospheric profiles, which are an important part of the error budget from ~ 35 km upwards (Steiner et al. 1999).

For the neutral atmosphere, we employed the ECHAM4 AGCM (Roeckner et al. 1999) in a new version including the middle atmosphere (MAECHAM – highest model level ~0.01hPa/~80km) at a resolution T42L39 (Manzini and McFarlane 1998). Two “time slice experiments” from 1995 to 2020 are run (currently ongoing), one including the transient anthropogenic forcings due to greenhouse gases, sulphate aerosols, and tropospheric ozone (“GAO run”), the other ignoring these forcings (“CTL run”). The two experiments were based, in terms of initial and boundary conditions and prescribed fields, on two recently completed ECHAM4 AOGCM long-term transient integrations at T42L19 resolution (“GSDIO run” and “CTL run”, respectively; see Roeckner et al. 1999 and Bengtsson et al. 1999 for details).

The GCM fields are stored every 6 hours over the full simulation period so that the subsequent simulations of occultation data can properly capture atmospheric variability from diurnal to decadal scales. Since the 39-level vertical domain extends up into the mesosphere (all other climate integrations we are aware of at \geq T42 resolution stop at ~10 hPa), reasonable middle atmosphere variability is captured as well, which is an important aspect for occultation simulations with realistic error characteristics. In our case only upward of ~0.035 hPa/~70km MSISE-90 climatology (Hedin 1991) is used.

Figure 1 illustrates an arbitrarily selected mid-July temperature field of the T42L39 runs.

For the ionosphere, we employ the NeUoG model (Leitinger et al. 1996), which is a global empirical 3D climatology model of the ionospheric electron density (and refractivity) field. In terms of temporal variability,

NeUoG accounts for diurnal, seasonal, and solar-activity dependences of the ionosphere. The suitability of the model for the present study has been confirmed recently by its high utility for several occultation-related studies (e.g., Leitinger and Kirchengast 1997).

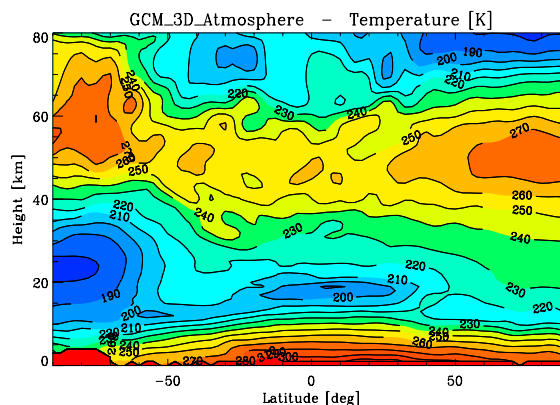


Figure 1: Latitude-height slice of temperature from a T42L39 GCM run (July 15, Yr02, 15 deg lon., 12 UT).

It is of particular importance to account for the ~11-yr solar activity dependence (forced by the F10.7 solar flux index in NeUoG), which maps into a decadal scale variability of ionospheric residual errors in occultation profiles. We use a dataset of daily F10.7 values spanning 1996 – 2020 (~ solar cycles 23 and 24), which essentially corresponds to the dataset available for cycles 21 and 22 (1976 – present). This furnishes quasi-realistic solar-activity forcing of the ionosphere from diurnal to decadal scales.

3.2 Simulation of Occultation Observables

Reflecting the typical layout of proposed next-generation occultation missions, such as the European ACE (Atmosphere Climate Experiment) mission, we assumed a constellation of six Low Earth Orbit (LEO) satellites, each equipped with an occultation receiver for acquiring GPS and GLONASS occultation events. Five missions, each with 5 years lifetime, are assumed to cover the 1996 – 2020 time period.

We restricted to setting occultations (sampling from ~90 km altitude downwards) received within an antenna beam width of ± 15 deg about the LEO orbit plane, since these are best qualified for climate purposes. This yields about 1000 occultation events per day. We utilize a small but reasonable subset of these only, in order to keep computing time at an affordable level: We further restrict to summer season (JJA) and to a 45 deg longitude (± 85 deg latitude) sector, respectively. The actual simulation of observables is then performed for ~ 1000 events per year, well distributed in space-time within the selected domain, for all 25 years and for both the “GAO run” and the “CTL run”, respectively.

For each event, the geometrical configuration (GNSS and LEO orbit arcs) is first computed based on proper Keplerian orbit elements. Second, the signal profile as seen by the sensor is simulated by means of

GNSS-to-LEO signal propagation through the atmosphere-ionosphere system (subsection 3.1) using a mm-precision 3D ray tracer. Finally, the “measured” excess phase path (and amplitude) profiles are simulated by modifying this signal profile with the effects of the instrument and raw-processing system such as precise-orbit-determination errors, antenna pattern, local multipath, receiver noise, and clock drifts.

The tool employed for these computations is a partially parallelized new version of the End-to-end GNSS Occultation Performance Simulator (EGOPS), which contains all required functionality and can simulate quasi-realistic observables (Kirchengast 1998). The simulation setup has been successfully validated using “testbed” GCM fields (cf. Fig. 1). The “operational” generation of the full simulated-observables database, which is besides the T42L39-GCM simulations the computationally most demanding part of the study, will thus start soon.

3.3 Temperature Profiles Retrieval

Based on the simulated-observables database, a database of retrieved temperature profiles will be produced, utilizing a well-tested retrieval chain recently implemented in the EGOPS tool as well. The algorithmic scheme is essentially the one of Syndergaard (1999) and is sketched in Figure 2 (the dry-air retrieval part applies).

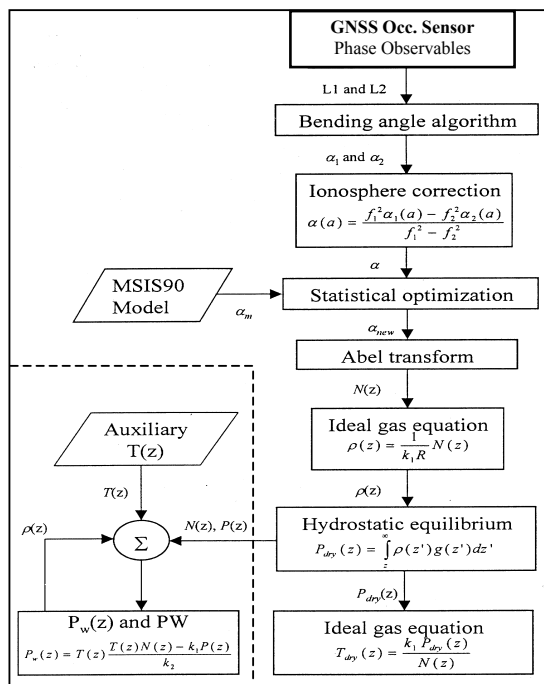


Figure 2: Retrieval scheme employed for temperature profile retrieval. (Based on drawing from P. Hoeg et al. 1998, priv. communications.)

Each excess phase profile is inverted, via a bending angle and a refractivity profile, to a (dry air)

temperature profile. Given the present focus, we ignore moisture and accept that the retrieved temperature profiles can be cold-biased up to ~ 8 km altitude (Kursinski et al. 1997).

Results of “testbed” retrievals indicate that rms errors of averages over 30 profiles are typically < 0.2 K below 35 km. Biases tend to depend on residual ionospheric errors and may exceed this level down into the lower stratosphere, but sufficient results are not yet available for any conclusion.

Our statistical analysis design with 17 latitudinal bins (see subsection 3.4) will yield ~ 55 – 60 profiles per statistical bin, given the ~ 1000 profiles per JJA sample (see subsection 3.2). This furnishes rms error suppression through averaging by a factor of ~7.5 against individual-profile rms errors, mitigating besides “instrumental” errors also “representativeness” errors due to limited sampling density.

3.4 Temperature Trend Analysis

Using the database of retrieved temperature profiles, a climatological “latitude-height slice” dataset, termed “measured” climatology, will be produced for each of the 50 JJA samples (25 years, 2 runs). 17 bins of 10 deg latitudinal width are used, with 34 height levels in each bin (within 2 – 50 km, core region 8 – 40 km), yielding a 17 x 34 matrix with a total of 578 values. For reference, the “true” climatology is computed on the same matrix based directly on the GCM temperature fields in the selected space-time domain. The difference of the two matrices is a direct indication of the total bias error associated with each matrix element.

Furthermore, for each bin the “true” profiles from the GCM fields are computed at all relevant occultation locations (~55–60 per bin) in order to estimate the rms and bias errors without the residual bias due to limited sampling density. These error estimates are again gathered on the same matrix as used above and are required for properly specifying the “measurement” error in the trend analysis scheme.

The trend analysis scheme is based on a multivariate weighted least-squares analysis approach and objectively assesses the linear temporal evolution, independently for each individual matrix element, of a series of up to 25 JJA climatology matrices (up to 25 years). Formally it reads

$$T_t = A_{fit} x_t + e_t \quad (1)$$

$$x_{fit} = S_{fit} A^T S_e^{-1} T \quad (2a)$$

$$S_{fit} = (A^T S_e^{-1} A)^{-1}, \quad (2b)$$

where Eq. (1) represents the fit design model (design matrix **A**), Eq. (2a) yields the best fit values (**x_{fit}**), and Eq. (2b) yields the covariance properties (**S_{fit}**), i.e., the fit error, respectively (**x**, fit-model parameter vector; **T**, temperature time series for given matrix element; **S_e**, covariance matrix of measured temperature series).

This scheme is, in particular, used to prepare matrices of the slope of fitted trend lines (fit-model parameter **x₁**) and of their standard deviations (square root of **S_{fit11}**). Such trend matrices (latitude-height slices)

will be produced for the “measured” and the “true” climatology, respectively, of both GCM runs. Roeckner et al. (1999) included indications of the magnitude of trends to be expected over the simulated period. The occultation observing system should be able to reliably detect such trends within ~ 20 years at least in some subspaces of the baselined latitude-height slice.

The temperature trend analysis tools are currently in the implementation phase.

3.5 Trend Detection Capability

The comparison of the trend and trend-error latitude-height slices from the “measured” climatologies of the “GAO run” and the “CTL run”, respectively, is of particular interest. These data allow to assess the capability of the observing system under study for detecting presumed antropogenically induced trends within the time period considered.

Statistical inference methods (hypothesis testing) will be employed for assessing trends over ~10 to 25 years, the lower bound depending on the trend results obtained.

The setup for this last study part is currently prepared and will be implemented upon completion of the trend analysis tools.

4. SUMMARY

We are analyzing the climate change monitoring potential, with focus on the atmospheric temperature change detection capability, of a GNSS occultation observing system by a realistic end-to-end observing system simulation experiment over the 25-yr period from 1996 to 2020. The implementation of the necessary tools as well as prerequisite simulations, in particular the novel T42L39-GCM simulations involved, are approaching completion by the end of 1999. We thus expect preliminary results early in 2000.

The main hypothesis under test is whether and to what degree a GNSS occultation observing system could monitor (anthropogenically driven) atmospheric change and consequently become a leading backbone of the Global Climate Observing System (GCOS).

The results are also of immediate interest for currently prepared research and demonstration missions such as the European ACE mission and the U.S./Taiwan COSMIC mission.

For the future we consider a study expansion extending the interest to how well a GNSS occultation observing system can aid attribution of climate change.

Acknowledgments. We are grateful to U. Schulzweida, U. Schlese, and M. Esch (MPIM Hamburg) for technical support and to E. Roeckner and J. Feichter (MPIM Hamburg) for fruitful discussions regarding the ECHAM4 GCM simulations. We are, furthermore, thankful to all our colleagues involved in the EGOPS development, especially S. Syndergaard (DMI Copenhagen), for contributing to this key tool of the study. The major financial support for the work is derived from the START-Programm No. Y103-CHE research award of the BM für Wissenschaft und Verkehr, Vienna, Austria.

REFERENCES

- Bengtsson, L., E. Roeckner, and M. Stendel, 1999: Why is the global warming proceeding much slower than expected? *J. Geophys. Res.*, **104**, 3865-3876.
- Gurvich, A. S., and T. G. Krasil'nikova, 1990: Navigation satellites for radio sensing of the Earth's atmosphere, *Sov. J. Remote Sensing*, **7**, 1124-1131.
- Hedin, A. E., 1991: Extension of the MSIS thermosphere model into the middle and lower atmosphere. *J. Geophys. Res.*, **96**, 1159-1172.
- IPCC, 1995: *The Science of Climate Change – Contribution of WG I to the 2nd assessment of the IPCC*. Cambridge Univ. Press, 572 pp.
- JSTC-GCOS, 1998: Report of the 7th session of the Joint Scientific and Technical Committee for GCOS. WMO/TD No. 857. [WMO, Geneva, Switzerland; avail. on-line via <http://www.wmo.ch> – GCOS.]
- Kirchengast, 1998: End-to-end GNSS Occultation Performance Simulator (EGOPS) overview and exemplary applications. *Wissenschaftl. Ber. No. 2/1998*, 138 pp. [Inst. for Meteorol. and Geophys., Univ. of Graz, Halbaerthg. 1, A-8010 Graz, Austria.]
- Kursinski, E. R., G. A. Hajj, K. R. Hardy, J. T. Schofield, and R. Linfield, 1997: Observing Earth's atmosphere with radio occultation measurements using the Global Positioning System. *J. Geophys. Res.*, **102**, 23429-23465.
- Leitinger, R., and G. Kirchengast, 1997: Inversion of the plasma signal in GNSS occultations – simulation studies and sample results. *Acta Geod. Geophys. Hung.*, **32**, 379-394.
- Leitinger, R., J. E. Titheridge, G. Kirchengast, and W. Rothleitner, 1996: A “simple” global empirical model for the F layer of the ionosphere (in German; English version avail. from corresponding author). *Kleinheubacher Ber.*, **39**, 697-704.
- Manzini, E., and N. A. McFarlane, 1998: The effect of varying the source spectrum of a gravity wave parameterization in a middle atmosphere GCM. *J. Geophys. Res.*, **103**, 31523-31539.
- Roeckner, E., L. Bengtsson, J. Feichter, J. Lelieveld, and H. Rodhe, 1999: Transient climate change simulations with a coupled atmosphere-ocean GCM including the tropospheric sulfur cycle. *J. Climate*, **12**, 3004-3032.
- Steiner, A. K., G. Kirchengast, and H. P. Ladreiter, 1999: Inversion, error analysis, and validation of GPS/MET occultation data. *Ann. Geophysicae*, **17**, 122-138.
- Syndergaard, S., 1999: Retrieval analysis and methodologies in atmospheric limb sounding using the GNSS radio occultation technique. Ph.D. thesis, 131 pp. [Danish Met. Institute, Lyngbyvej 100, D-2100 Copenhagen, Denmark.]
- Ware, R., et al., 1996: GPS sounding of the atmosphere from Low Earth Orbit: Preliminary results. *Bull. Am. Meteorol. Soc.*, **77**, 19-40.